DOI: 10.1002/chem.200601619

The Phenalenyl Motif: A Magnetic Chameleon

Michał K. Cyrański,[a] Remco W. A. Havenith,[b, f] Michał A. Dobrowolski,[a] Benjamin R. Gray,[c] Tadeusz M. Krygowski,[a] Patrick W. Fowler,*[d] and Leonardus W. Jenneskens*[e]

Abstract: The 12π cation (**3**) and 14π anion (**4**) derived from the phenalenyl radical (**2**) support diatropic ("aromatic") perimeter ring currents, but isoelectronic replacement of the central atom by either boron (**5**) or nitrogen (**6**) leads to paratropic ("antiaromatic") current; the ipsocentric approach to molecular magnetic response accounts for all four patterns in terms of competition between translationally and rotationally allowed virtual π–π* excitations.

Keywords: ab initio calculations · aromaticity · Hückel theory · phenalenes · ring currents

Introduction

The 13-carbon-phenalene motif (Figure 1), in which three hexagonal rings are fused at a central vertex (position 10), is chemically versatile.[1] Phenalene (**1**) itself gives access to π-conjugated polycyclic compounds by hydrogen abstraction (to the $C_{13}H_9$ 13π phenalenyl radical, **2**), hydride abstraction (to the $C_{13}H_9$ 12π phenalenyl cation, **3**) or deprotonation (to the $C_{13}H_9$ 14π phenalenyl anion, **4**) with applications in ma-

[a] Dr. M. K. Cyrański, M. A. Dobrowolski, Prof. Dr. T. M. Krygowski
Department of Chemistry, University of Warsaw
Pasteura 1, 01–093 Warsaw (Poland)

[b] Dr. R. W. A. Havenith
Theoretical Chemistry Group, Utrecht University
Padualaan 8, 3584 CH Utrecht (The Netherlands)

[c] B. R. Gray
School of Chemistry, University of Nottingham
University Park, Nottingham, NG7 2RD (UK)

[d] Prof. Dr. P. W. Fowler
Department of Chemistry, University of Sheffield
Sheffield S3 7HF (UK)
Fax: (+44) 114-222-9346
E-mail: P.W.Fowler@sheffield.ac.uk

[e] Prof. Dr. L. W. Jenneskens
Organic Chemistry and Catalysis, Utrecht University
Padualaan 8, 3584 CH Utrecht (The Netherlands)
Fax: (+31) 302-534-533
E-mail: l.w.jenneskens@chem.uu.nl

[f] Dr. R. W. A. Havenith
Affiliated to Organic Chemistry and Catalysis
Utrecht University
Padualaan 8, 3584 CH Utrecht (The Netherlands)

Supporting information for this article is available on the WWW under http://www.chemeurj.org/ or from the author.

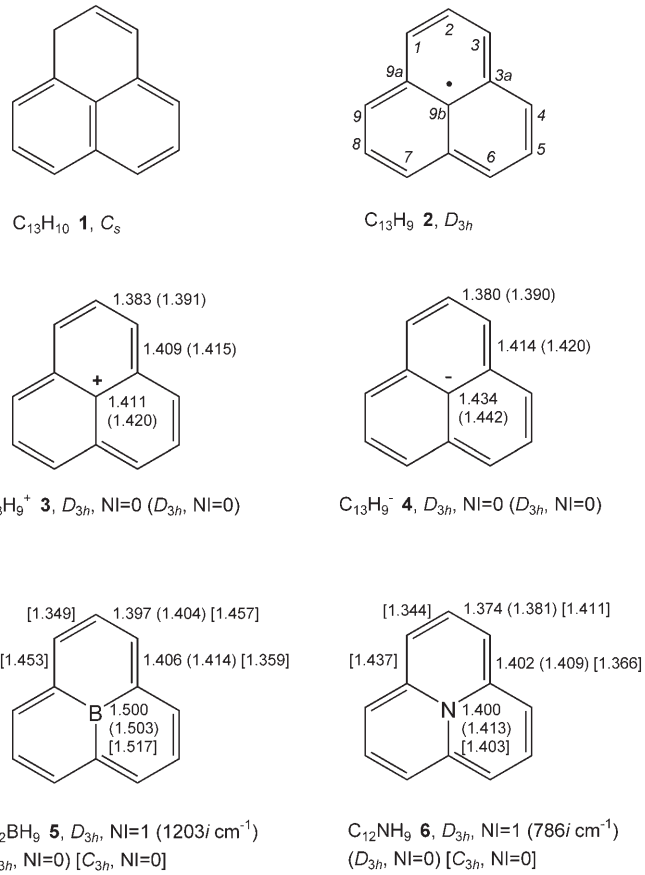

$C_{13}H_{10}$ **1**, C_s

$C_{13}H_9$ **2**, D_{3h}

$C_{13}H_9^+$ **3**, D_{3h}, NI=0 (D_{3h}, NI=0)

$C_{13}H_9^-$ **4**, D_{3h}, NI=0 (D_{3h}, NI=0)

$C_{12}BH_9$ **5**, D_{3h}, NI=1 (1203*i* cm^{-1}) (D_{3h}, NI=0) [C_{3h}, NI=0]

$C_{12}NH_9$ **6**, D_{3h}, NI=1 (786*i* cm^{-1}) (D_{3h}, NI=0) [C_{3h}, NI=0]

Figure 1. Phenalene-related molecules. RHF/6-31G** D_{3h} constrained structures are illustrated for **3**–**6**, with NI equal to the number of imaginary frequencies. B3LYP/6-311G** results are shown in parentheses, and RHF/6-31G** results for C_{3h} **5** and **6** are shown in square brackets. (Geometries calculated with the B3LYP/6-31G** basis set show only minor differences.)

terials science.[2] It is a truism that, as an odd π-electron molecule, the 13π-electron phenalenyl radical (**2**) lies between 4N and 4N+2 π-conjugated systems, but although naïve π-electron counting based on this fact would suggest markedly different behaviour for the phenalenyl cation (12π, **3**) and anion (14π, **4**),[3] we show here that both the cation (**3**) and anion (**4**) are predicted to sustain well-defined diatropic perimeter ring currents, traditionally a sign of aromaticity on the magnetic criterion.[4] In contrast, the respective isoelectronic analogues, in which the central carbon atom of the phenalenyl motif is replaced by a boron ($C_{12}BH_9$, 9b-boraphenalene, **5**) or nitrogen atom ($C_{12}NH_9$, 9b-azaphenalene, **6**, also known as cycl[3.3.3]azine) (Figure 1), are both predicted to sustain strong paratropic perimeter ring currents, a sign of antiaromaticity on the magnetic criterion. These predictions, based on the application of ab initio current density mapping by using the well-established ipsocentric approach,[5–7] are foreshadowed in some earlier studies of properties of **3**–**6**.[8] These predictions can be given a clear rationale, once the importance of factors of molecular topology, orbital symmetry and orbital energy,[9] as opposed to raw π-electron count, are recognized. Manipulation of these factors should allow tuning of molecular properties in related functionalized-phenalenyl derivatives and hetero-atom containing analogues, with implications for molecular design. In this paper we treat the following closed-shell systems: the 12π-electron phenalenyl cation (**3**), the 14π-electron phenalenyl anion (**4**), and their heterocyclic analogues, 9b-boraphenalene (**5**, 12π) and 9b-azaphenalene (**6**, 14π). The nitrogen analogue, 9b-azaphenalene, has been synthesised[10] and found to be chemically reactive, undergoing facile addition,[11] oxidation and reduction.[12] In line with the maps of induced ring currents that we will show, 9b-azaphenalene exhibits strong paratropic shifts in its ^{1}H NMR signals.[10,13]

Results and Discussion

Optimised structures for the systems studied in the present work are shown in Figure 1. Computed π-current-density maps for the phenalenyl cation (**3**), the phenalenyl anion (**4**), and their heterocyclic analogues, 9b-boraphenalene (**5**) and 9b-azaphenalene (**6**) are shown in Figure 2. These were calculated by using our standard procedure of optimisation of geometry at the RHF/6-31G** level,[14,15] followed by ipsocentric CTOCD-DZ/6-31G**//RHF/6-31G** calculation[16] of the current induced by a magnetic field perpendicular to the plane of the nuclei. Structures were initially constrained to D_{3h} symmetry, and the status of the stationary point checked by diagonalisation of the Hessian. These were the structures used in the construction of Figure 2. At the RHF/6-31G** level, D_{3h} structures of **3** and **4** are true minima, whereas both **5** and **6** are transition states (with a single imaginary frequency); **5** and **6** both relax to C_{3h} minima. At the B3LYP/6-31G** and B3LYP/6-311G** levels, all four systems (**3**–**6**) gave true minima in D_{3h} symmetry (Figure 1)

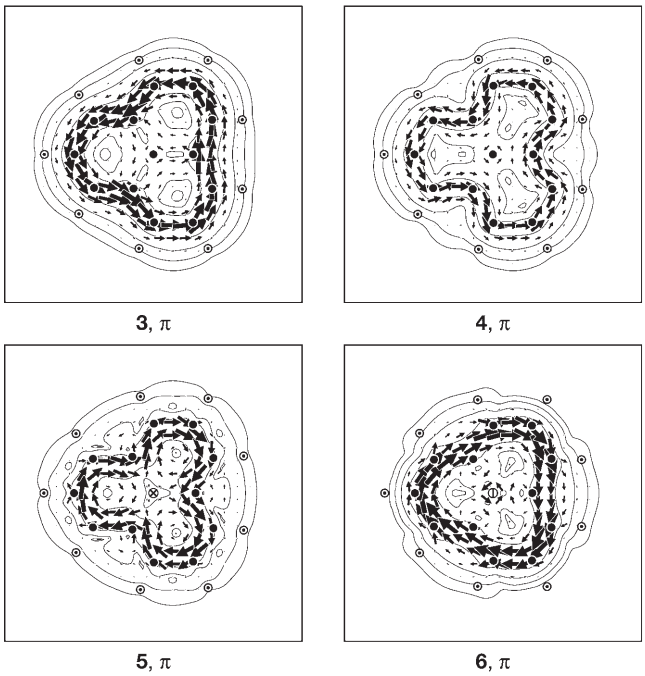

Figure 2. Current-density maps for response to a perpendicular external magnetic field of the π systems of ions **3** and **4** and molecules **5** and **6**, calculated at the CTOCD-DZ/6-31G**//RHF/6-31G** level (D_{3h} constrained) and plotted in the plane $1a_0$ above that of the nuclei. Vectors indicate direction and intensity of the in-plane current and contours/shading the total magnitude. Anticlockwise (clockwise) circulations represent diatropic (paratropic) ring currents.

and hence the C_{3h} minima for **5** and **6** may be examples of spurious symmetry breaking at the restricted Hartree–Fock (RHF) level, as observed in calculations on porphyrins and related macrocyclic systems.[17] The continuous set of gauge transformations (CSGT) method (CSGT) at the B3LYP/6-311G** level was used for the calculation of the exaltation of magnetic susceptibility, at geometries optimised at the same level of theory. GIAO/B3LYP/6-311G** calculations were used for nucleus-independent chemical-shift (NICS) calculations and the harmonic oscillator model of aromaticity (HOMA) values were based on B3LYP/6-311G** optimal geometries.

Maps were plotted for both RHF and DFT D_{3h} structures (**3**–**6**) and also for RHF C_{3h} structures for **5** and **6** (see the Supporting Information). As the essential features of the maps were found to be independent of the choice of RHF or DFT geometry and of D_{3h} or C_{3h} symmetry, we illustrate here only the RHF/6-31G** D_{3h} (minimal and constrained) maps (Figure 2). These maps show induced current in the plotting plane $1a_0$ above that of the nuclei, with vectors indicating direction and intensity of the in-plane current and contours/shading indicating the total magnitude. Anticlockwise (clockwise) circulations represent diatropic (paratropic) ring currents. As mentioned in the introduction, the maps show well-marked diatropic π currents for **3** and **4**, but paratropic π currents for **5** and **6**. Experimental evidence from ^{1}H and internal ^{13}C chemical shifts[8b,c] is in line with the ob-

servation that 4N+2 (**4**) has a weaker calculated diatropic perimeter current than 4N (**3**).

If we believe in π-electron counting, the fact that 4N/4N+2 phenalenyl ions **3** and **4** both sustain strong diatropic perimeter circulations is counterintuitive, although it is a direct consequence of the alternant nature of the carbon framework[8b] that anion and cation should have similar currents (in a graph-theoretical Hückel–London approach, with a fixed underlying geometry, the currents would be identical in **3** and **4**). Equally perplexing would be the reversal of current on isoelectronic replacement: the 12π cation (**3**, a 4N system) sustains a diatropic circulation, whereas its bora-analogue (**5**) possesses a paratropic circulation; conversely, although the 14π-electron (4N+2) phenalenyl anion system (**4**) is diatropic as expected on electron count, its isoelectronic aza-analogue (**6**) is paratropic.

Other measures of aromaticity[18] also fail to distinguish significantly between **3** and **4**, and between **5** and **6** (see Table 1). Perimeter bond-length alternation is similar for **3** and **4**, and the geometric HOMA[19] indices are consequently similar for these 12π and 14π species; the phenalene cation (**3**), apparently having more efficient perimeter π-electron delocalisation. The perimeters of **5** and **6** are again similar in their degree of alternation, and the HOMA index shows little difference between the two heterocyclic systems, or between them and the carbocycles (**3** and **4**), telling us nothing about aromaticity/antiaromaticity beyond an indication of strong delocalisation for all four species.

Table 1. Indicators of aromaticity/antiaromaticity for the phenalene-related species **3**–**6**. These are magnetic (NICS(0), NICS(1), Λ), energetic (ASE), and geometric (HOMA) applied to the perimeter bonds, as described in the text.

	3	**4**	**5**	**6**
NICS(0) [ppm]	−3.9	−0.7	+20.8	+22.6
NICS(1) [ppm]	−7.8	−3.9	+14.5	+16.0
Λ [cgs ppm]	+23.3	+5.9	−54.1	−66.0
ASE [kcal mol^{-1}]	34.5	30.8	15.8	21.4
perimeter HOMA	0.905	0.868	0.880	0.937

The aromatic stabilisation energies (ASE),[20] based here on comparison of the total energies of a methylated reference molecule and its formally localized exocyclic methylene isomer [see Eq. (1)],[21] do not differentiate strongly between the 12π and 14π systems: all four systems have a positive stabilisation energy, even if ASE of the phenalene cation (**3**) and phenalene anion (**4**) are higher than those of 9b-boraphenalene (**5**) and 9b-azaphenalene (**6**).

The NICS,[22] computed at ring centres and at 1 Å above (NICS(0) and NICS(1)[23]) indicate diatropicity for the rings in **3** and **4** and paratropicity for the rings in **5** and **6**, and again show no strong dependence on electron count. Exaltation of magnetic susceptibility (Λ),[24] as estimated from Equation (1), picks up the difference between the carbocyclic systems with diatropic π current (positive values of Λ), and heterocyclic systems with paratropic π current (negative values of Λ), but again does not distinguish 12π/14π systems.

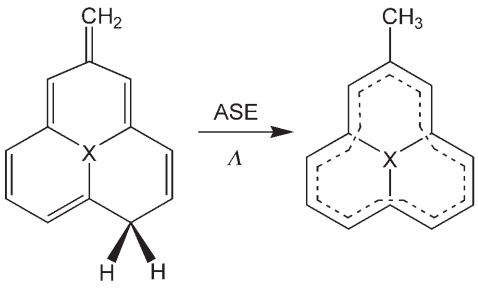

(1)

Thus, all three magnetic indicators of aromaticity/antiaromaticity are broadly consistent. If the currents are as predicted in Figure 2, then the π contributions to the out-of-plane components of the central shielding tensor and the magnetisability tensor are explained. The question then remains: why do the currents have the observed sense, and a strong dependence on the central atom, but not on the π-electron count?

The ipsocentric approach, with its well-defined partition of current into orbital contributions,[7] gives a framework for prediction of current sense and intensity. Diatropic and paratropic currents are predicted by symmetry-based selection rules, in which initial excitation from an occupied orbital gives a diatropic contribution to current if the product of occupied and unoccupied orbital symmetries contains that of an in-plane translation, and paratropic if the product contains the symmetry of an in-plane rotation. The contribution of a particular excitation is moderated by the difference in energy of initial (occupied) and final (unoccupied) orbitals.

The first step in interpreting the π maps is to partition the current-density contributions between the various occupied orbitals. Current-density maps of the contributions of the frontier orbitals to the total π current in the two systems **3** and **4** are shown in Figure 3, and those for their hetero-atom analogues (**5** and **6**) are shown in Figure 4. The diatropic perimeter current in the phenalenyl cation (**3**) arises from the contribution of the doubly degenerate 2e″ HOMO, and in the phenalenyl anion (**4**) from the 2e″ HOMO-2 pair, supplemented by the $2a_2''$ HOMO−1. In the heterocyclic systems, in contrast, the main contribution is a paratropic current from the non-degenerate HOMO (which has a_2'' symmetry in the case of **5** and a_1'' symmetry in the case of **6**), moderated by a minor diatropic contribution from the e″ HOMO−1.

Figure 5 illustrates schematically the RHF/6-31G** calculated frontier orbitals, their energy levels and the allowed virtual excitations between them, for the phenalenyl cation (**3**), the phenalenyl anion (**4**), and their heterocyclic analogues, 9b-boraphenalene (**5**) and 9b-azaphenalene (**6**). The similarity of the current-density maps between cation (**3**) and anion (**4**), and their difference from those for the related heteroatom systems (**5** and **6**) are both rationalised by

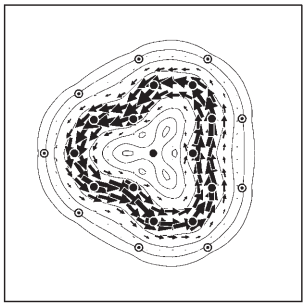

3, 2e" (HOMO)

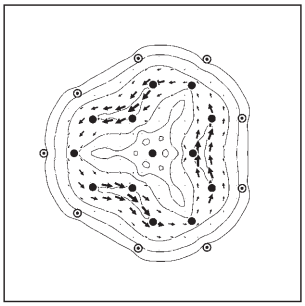

4, 2e" (HOMO-2)

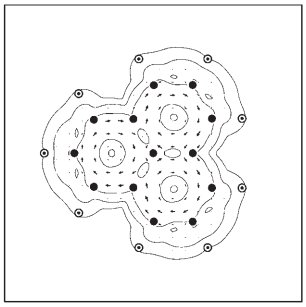

3, $2a_2$" (HOMO-1)

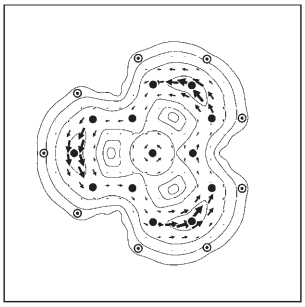

4, $2a_2$" (HOMO-1)

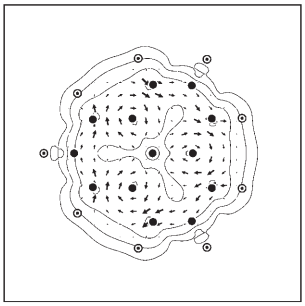

4, $1a_1$" (HOMO)

Figure 3. Maps of π frontier-orbital contributions to current density for **3** and **4**. Methods and plotting conventions as Figure 2.

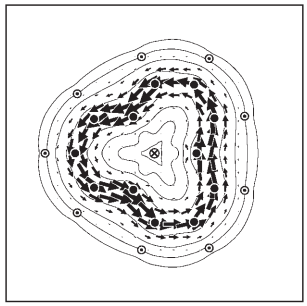

5, 2e" (HOMO-1)

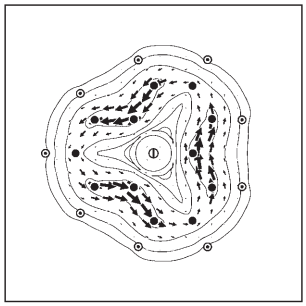

6, 2e" (HOMO-1)

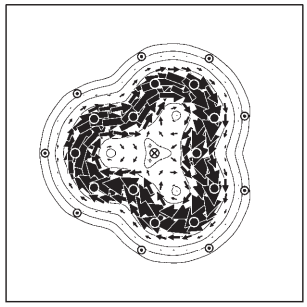

5, $2a_2$" (HOMO)

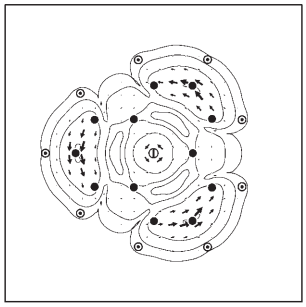

6, $2a_2$" (HOMO-2)

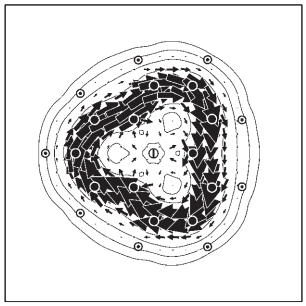

6, $1a_1$" (HOMO)

Figure 4. Maps of π frontier-orbital contributions to current density for **5** and **6**. Methods and plotting conventions as Figure 2.

the product symmetries and the trends in the orbital energies. In the carbocyclic systems (**3** and **4**), the dominant excitations originating from the e″ orbitals are translationally allowed, and the rotationally allowed a_2''–a_1'' excitation ($2a_2''\rightarrow 1a_1''$, cation **3**, $1a_1''\rightarrow 3a_2''$, anion **4**) plays only a minor role. In the heterocyclic systems **5** and **6**, the HOMO–LUMO gap shrinks and the current is increasingly dominated by the paratropic excitation.

As the orbital currents depend essentially on symmetry and the variation of orbital energy with electronegativity, they should already be explained by a simple analytical representation of the π systems of **3**–**6**. In simple Hückel theory, all carbon centres are assigned a coulomb integral α and all bonds are assigned a resonance integral β. The nature of the central atom is taken into account by assigning it a coulomb integral $\alpha+\eta\beta$, in which η is an electronegativity parameter (B would usually have $\eta\approx -1.0$ and planar N $\eta\approx +1.5$[25]). The energy levels are then determined, to within a shift of origin α and a scale $|\beta|$, by the eigenvalues $\{\lambda\}$ of a 13×13 matrix which factors into $a_1''+4a_2''+4e''$ blocks. The carbocycle has a symmetric energy-level diagram, and the diagrams for $+\eta$ and $-\eta$ are related by reversing the energy scale (Figure 6). Symmetry considerations show that the non-bonding a_1'' and four $4e''$ levels must be independent of η (they are unchanged levels of the perimeter[12]cycle), whereas the $4a_2''$ levels, two bonding and two antibonding, are determined by roots of a quartic [Eq. (2)].

$$\lambda^4 - \eta\lambda^3 - 7\lambda^2 + 4\eta\lambda + 6 = 0. \qquad (2)$$

The HOMO–LUMO gap, Δ, lies between the second a_2'' and non-bonding orbital (NBO) levels (12π), or the NBO and third a_2'' levels (14π), with the consequence that $\Delta(12\pi, \eta=-\delta)=\Delta(14\pi, \eta=+\delta)$, and in particular, Δ is equal (and maximal) for the phenalenyl cation (**3**) and anion (**4**). As $|\eta|$ goes from 0 to 1, the gap varies smoothly from 1 to $\sqrt{3}-1\approx 0.732$ in units of $|\beta|$. In the high-$|\eta|$ limit, the four roots of the quartic tend asymptotically to η, 0, ± 2, corresponding to a physical situation in which there is a level $\alpha+$

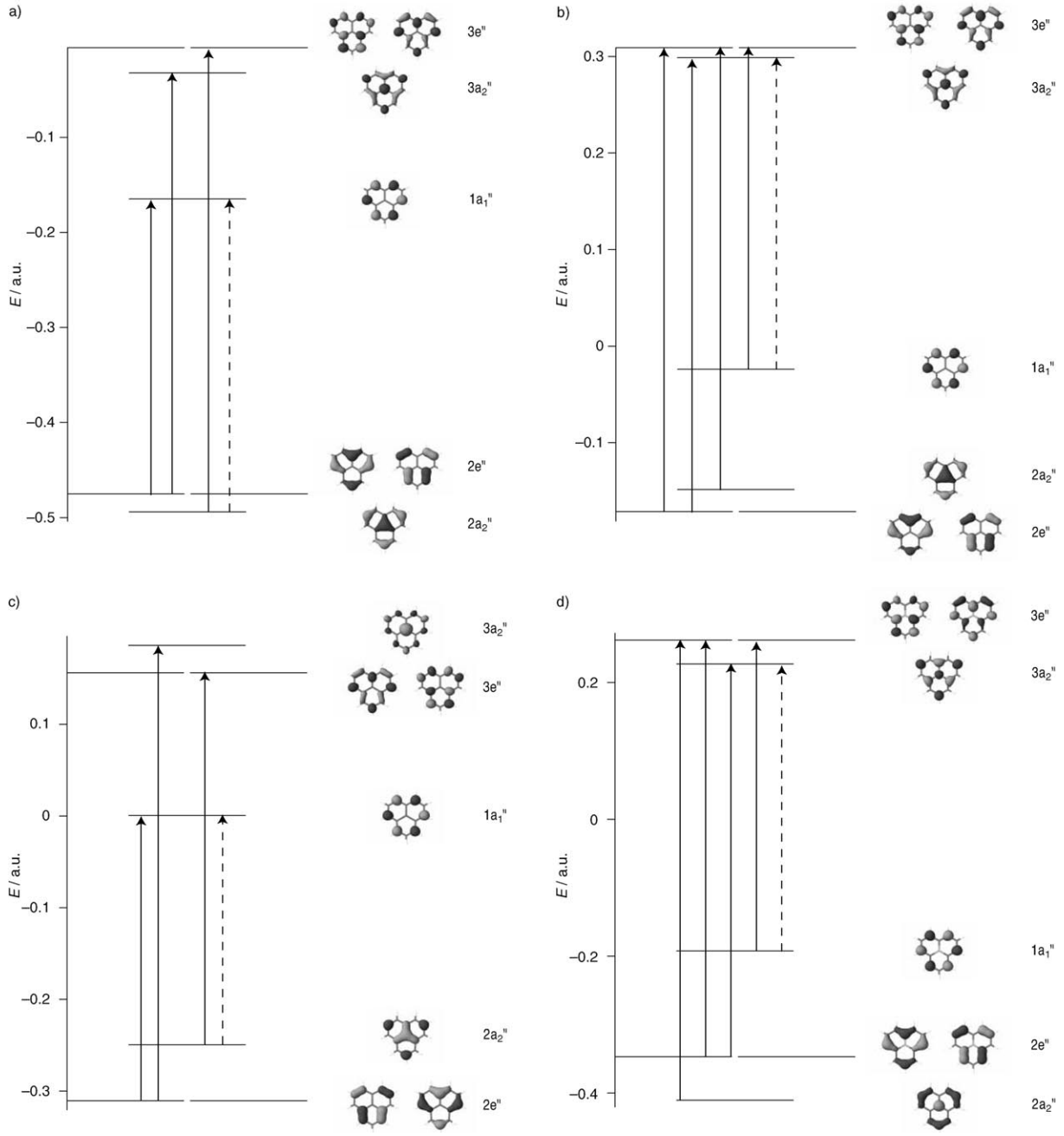

Figure 5. a)–d) Frontier orbitals, energy levels and virtual excitations for the phenalene-related systems **3**–**6**, respectively. The main translationally (rotationally) allowed excitations are indicated by full (dashed) arrows. All arrows start from occupied and end on empty orbitals.

$\eta\beta$ that either contains two electrons ($\eta\rightarrow+\infty$) or is empty ($\eta\rightarrow-\infty$), and is decoupled from the other levels, which, therefore, return to the [12]-annulene energies of α, $\alpha\pm2\beta$.

Significantly for the ipsocentric explanation of the currents, the $\eta\leftrightarrow-\eta$ symmetry properties of the energy-level diagram also imply that virtual excitations across the gap have the same symmetries in 12π and 14π systems: for both electron counts, the HOMO–LUMO symmetry product is a_2' (rotational), whereas HOMO–(LUMO+1) and (HOMO−1)–LUMO products are e′ (translational), with accidental degeneracy at $\eta=0$. The different patterns of current then arise from the balance between these virtual excitations. Comparison of Figures 5 and 6 shows that Hückel theory gives a close overall match to the ab initio descriptions of the frontier orbitals, their relative energies and symmetries. The driver of the change from diatropic (**3** and **4**) to paratropic (**5** and **6**) current is seen to be the variation with η of the HOMO–LUMO gap: as η changes from the

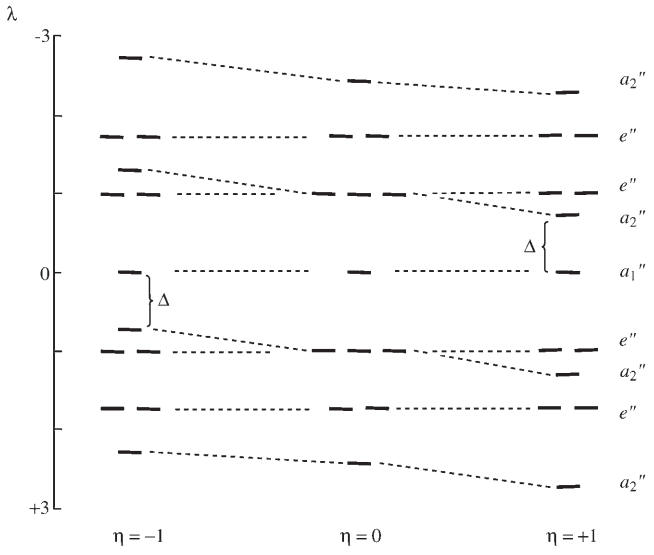

Figure 6. Hückel π-energy levels for systems **3**–**6**, labeled by symmetry. The numbers on the vertical scale indicate the dimensionless eigenvalue Λ, from which orbital energies follow as $\varepsilon = \alpha + \eta\beta$. Λ_1 to Λ_4 are roots of a quartic [Eq. (2)], and are illustrated here for $\eta = \pm 1$.

carbon value in either direction, the a_2''–a_1'' gap shrinks, and the current is increasingly dominated by the paratropic excitation. This explains the maps.

In line with the rationalisation of currents in terms of Hückel theory, it is notable that a pseudo-π[26] treatment, in which each carbon atom bearing a p_π orbital is replaced by a pseudo-hydrogen atom, reproduces essentially exactly the cation and anion maps and their orbital decomposition. Subtleties of the adaptation of the pseudo-π method for heteroatoms have been discussed elsewhere.[27]

In passing, we may note that the ipsocentric method gives a direct interpretation of the maps as they are seen, that is, it interprets the perimeter current. In contrast, graph-theoretical models that decompose the current into circuit contributions[28,8b] would interpret the plotted perimeter current as a summation of superimposed diatropic benzene- and naphthalene-circuit contributions that cancel out everywhere except on the perimeter, plus a weak paratropic perimeter-circuit contribution. Each perimeter edge belongs to one 6-ring, two 10-rings and one 12-ring in this decomposition. This account in terms of cancellations now seems unnecessarily indirect, if ipsocentric orbital contributions can show the perimeter current as a single unified object arising directly from the perturbation of the two HOMO electrons by the applied field.

The magnetic indicators Λ and NICS should follow the ring currents, as noted earlier. The poor behaviour of the other potential indicator of aromaticity, HOMA, is also consistent with the Hückel energy-level diagram, in that the 12π and 14π systems differ by occupation of a non-bonding orbital: by definition, molecular geometry is insensitive to occupancy of the NBO.

A bonus of an orbital-based model of these systems is that it gives a straightforward prediction for the properties of the 13π radical (**2**). In the simplest approximation,[29] the orbital current in the radical should be the average of the cationic and anionic currents, so the species **2** should also exhibit a significant diatropic perimeter current. (The net spin of the odd-electron species will also give rise to a first-order coupling with the external-magnetic field.)

Conclusion

Understanding of the variation of physical properties with structure and electron count is important for the applications of phenalenyl systems (**2**–**4**) (and the potential applications of their heteroatom analogues (**5**–**6**)) in materials science. The phenalenyl motif provides a clear case in which electron counting alone is not informative about magnetic response, but equally, chemical considerations of orbital symmetry and energy, allied to the ipsocentric analysis, can give design criteria for rationalisation and prediction of π current-density patterns and concomitant aromaticity.

Acknowledgements

P.W.F. thanks the Royal Society/Wolfson Research Merit Award Scheme for financial support. R.W.A.H. acknowledges the Netherlands Organisation for Scientific Research (NWO, grant 700.53.401 and NWO/NCF, project SG-032). M.K.C. and T.M.K. thank Edyta Pindelska for starting geometries of the phenalene systems. M.K.C. acknowledges grant 120000–501/68-BW-1681/2/05 for financial support. The Interdisciplinary Centre for Mathematical and Computational Modelling (Warsaw) is acknowledged for providing computational facilities.

[1] P. J. Garratt, *Aromaticity*, John Wiley & Sons, New York, **1986**.
[2] a) V. Boelkelheide, C. E. Larrabee, *J. Am. Chem. Soc.* **1950**, *72*, 1245–1249; b) D. H. Reid, *Tetrahedron* **1958**, 3, 339–352; c) R. Pettit, *J. Am. Chem. Soc.* **1960**, *82*, 1972–1975; d) D. H. Reid, *Q. Rev., Chem. Soc.* **1965**, *19*, 274–302; e) K. Goto, T. Kubo, K. Yamamoto, K. Nakasuji, K. Sato, D. Shiomi, T. Takui, M. Kubato, T. Kobayashi, K. Yakusi, J. Ouyang, *J. Am. Chem. Soc.* **1999**, *121*, 1619–1620; f) P. A. Koutentis, Y. Chen, Y. Cao, T. P. Best, M. E. Itkis, L. Beer, R. T. Oakley, A. W. Cordes, C. P. Brock, R. C. Haddon *J. Am. Chem. Soc.* **2001**, *123*, 3864–3871; g) V. I. Kovalenko, A. R. Khamatgalimov, *Chem. Phys. Lett.* **2003**, *377*, 263–268; h) S. Zheng, J. Lan, S. I. Khan, Y. Rubin *J. Am. Chem. Soc.* **2003**, *125*, 5786–5791.
[3] a) E. Hückel, *Z. Phys.* **1931**, *76*, 204–286; b) V. I. Minkin, M. N. Glukhovstev, B. Ya. Simkin, *Aromaticity and Antiaromaticity: Electronic and Structural Aspects*, John. Wiley, New York, **1994**.
[4] P. Lazzeretti, *Phys. Chem. Chem. Phys.* **2004**, *6*, 217–223.
[5] T. A. Keith, R. F. W. Bader, *Chem. Phys. Lett.* **1993**, *210*, 223–231.
[6] S. Coriani, P. Lazzeretti, M. Malagoli, R. Zanasi, *Theor. Chim. Acta* **1994**, *89*, 181–192.
[7] E. Steiner, P. W. Fowler, *J. Phys. Chem. A.* **2001**, *105*, 9553–9562.
[8] a) M. J. S. Dewar, N. Trinajstić, *J. Chem. Soc. A* **1969**, 1754–1755; b) I. Sethson, D. Johnels, U. Elflund, A. Sygula, *J. Chem. Soc. Perkin Trans. 2* **1990**, 1339–1341; c) H. Prinzbach, V. Freudenberger, and U. Scheidegger, *Helv. Chim. Acta* **1967**, *50*, 1087–1107.
[9] a) E. Steiner and P. W. Fowler, *Chem. Commun.* **2001**, 2220–2221; b) E. Steiner, P. W. Fowler, *Phys. Chem. Chem. Phys.* **2004**, *6*, 261–272.
[10] a) D. Farquhar, D. Leaver, *J. Chem. Soc. D*, **1969**, 24–25; b) D. Farquhar, T. Gough, D. Leaver, *J. Chem. Soc. Perkin Trans. 1* **1976**, 341–355.

[11] For reviews, see a) Y. Matsuda, H. Gotou, *Heterocycles* **1987**, *26*, 2757–2772, and references therein. b) Y. Matsuda, *Yakugaku Zasshi* **2001**, *121*, 971–988, and references therein.
[12] For example, see a) F. Gerson, J. Jachimowicz, D. Leaver, *J. Am. Chem. Soc.* **1973**, *95*, 6702–6708; b) M. H. Palmer, D. Leaver, J. D. Nesbet, R. W. Millar, R. Edgell, *J. Mol. Struct.* **1977**, *42*, 85–101.
[13] a) R. C. Haddon, *Tetrahedron* **1972**, *28*, 3613–3633; b) R. C. Haddon, *Tetrahedron* **1972**, *28*, 3635–3655.
[14] M. J. Frisch, G. W. Trucks, H. B. Schlegel, G. E. Scuseria, M. A. Robb, J. R. Cheeseman, J. A. Montgomery, Jr., T. Vreven, K. N. Kudin, J. C. Burant, J. M. Millam, S. S. Iyengar, J. Tomasi, V. Barone, B. Mennucci, M. Cossi, G. Scalmani, N. Rega, G. A. Petersson, H. Nakatsuji, M. Hada, M. Ehara, K. Toyota, R. Fukuda, J. Hasegawa, M. Ishida, T. Nakajima, Y. Honda, O. Kitao, H. Nakai, M. Klene, X. Li, J. E. Knox, H. P. Hratchian, J. B. Cross, C. Adamo, J. Jaramillo, R. Gomperts, R. E. Stratmann, O. Yazyev, A. J. Austin, R. Cammi, C. Pomelli, J. W. Ochterski, P. Y. Ayala, K. Morokuma, G. A. Voth, P. Salvador, J. J. Dannenberg, V. G. Zakrzewski, S. Dapprich, A. D. Daniels, M. C. Strain, O. Farkas, D. K. Malick, A. D. Rabuck, K. Raghavachari, J. B. Foresman, J. V. Ortiz, Q. Cui, A. G. Baboul, S. Clifford, J. Cioslowski, B. B. Stefanov, G. Liu, A. Liashenko, P. Piskorz, I. Komaromi, R. L. Martin, D. J. Fox, T. Keith, M. A. Al-Laham, C. Y. Peng, A. Nanayakkara, M. Challacombe, P. M. W. Gill, B. Johnson, W. Chen, M. W. Wong, C. Gonzalez, J. A. Pople, Gaussian, Inc., Wallingford, CT, **2004**.
[15] M. F. Guest, I. J. Bush, H. J. J. van Dam, P. Sherwood, J. M. H. Thomas, J. H. van Lenthe, R. W. A. Havenith, J. Kendrick, *Mol. Phys.* **2005**, *103*, 719–747.
[16] P. Lazzeretti, R. Zanasi, *SYSMO Package*, University of Modena, Modena, Italy, **1980**, with additional routines by E. Steiner, P. W. Fowler, R. W. A. Havenith, A. Soncini.
[17] a) P. M. Kozlowski, M. Z. Zgierski, J. Baker, *J. Chem. Phys.* **1998**, *109*, 5905–5913; b) E. Steiner, P. W. Fowler, *Org. Biomol. Chem.* **2003**, *1*, 1785–1789.
[18] T. M. Krygowski, M. K. Cyrański, Z. Czarnocki, G. Hafelinger, A. R. Katritzky, *Tetrahedron* **2000**, *56*, 1783–1796.
[19] a) T. M. Krygowski, *J. Chem. Inf. Comput. Sci.* **1993**, *33*, 70–78; b) T. M. Krygowski, M. Cyrański, *Tetrahedron* **1996**, *52*, 1713–1722; c) T. M. Krygowski, M. K. Cyrański, *Chem. Rev.* **2001**, *101*, 1385–1419. HOMA (Harmonic Oscillator Model of Aromaticity) is defined as follows: $\mathrm{HOMA}=1-\frac{\alpha}{N}\sum (R_{opt}-R_i)^2$, in which N is the number of bonds of individual lengths R_i taken into the summation; here α (not to be confused with the Hückel coloumb integral) is an empirical constant fixed to give $\mathrm{HOMA}=0$ for a model non-aromatic system and 1 for a system with all bonds equal to an optimal value R_{opt}, assumed to be realised for a fully aromatic system.
[20] M. K. Cyrański, *Chem. Rev.* **2005**, *105*, 3773–3811.
[21] P. von R. Schleyer, F. Pühlhofer, *Org. Lett.* **2002**, *4*, 2873–2876.
[22] NICS, a magnetism-based measure of aromaticity, is defined as the negative value of the absolute shielding calculated at a ring center (NICS(0)) or at 1 Å above it (NICS(1)). Rings with negative NICS values are said to be aromatic.[23]
[23] a) P. von R. Schleyer, C. Maerker, A. Dransfeld, H. Jiao, N. J. R. van Eikema Hommes, *J. Am. Chem. Soc.* **1996**, *118*, 6317–6318; b) For a review see: Z. Chen, C. S. Wannere, C. Corminboeuf, R. Puchta, P. von R. Schleyer, *Chem. Rev.* **2005**, *105*, 3842–3888.
[24] a) H. J. Dauben, J. D. Wilson, J. L. Laity, *J. Am. Chem. Soc.* **1968**, *90*, 811–813; b) H. J. Dauben, J. D. Wilson, J. L. Laity, *J. Am. Chem. Soc.* **1969**, *91*, 1991–1998; c) H. J. Dauben, J. D. Wilson, J. L. Laity in *Non-Benzenoid Aromatics, Vol. 2*. (Ed.: J. P. Snyder), Academic Press, New York, **1971**, and references therein; d) P. von R. Schleyer, H. Jiao, *Pure Appl. Chem.* **1996**, *68*, 209–218.
[25] A. Streitwieser, Jr., *Molecular Orbital Theory for Organic Chemists*, Wiley, New York, **1962**.
[26] P. W. Fowler and E. Steiner, *Chem. Phys. Lett.* 2002, 364, 259–266.
[27] A. Soncini, C. Domene, J. J. Engelberts, P. W. Fowler, A. Rassat, J. H. van Lenthe, R. W. A. Havenith and L. W. Jenneskens, *Chem. Eur. J.* **2005**, *11*, 1257–1266.
[28] J. Aihara, *J. Am. Chem. Soc.* **2006**, *128*, 2873–2879.
[29] a) P. W. Fowler, E. Steiner, L. W. Jenneskens, *Chem. Phys. Lett.* **2003**, *371*, 719–723; b) V. Gogonea, P. von R. Schleyer, P. R. Schreiner, *Angew. Chem.* **1998**, *110* 2045–2049; *Angew. Chem. Int. Ed.* **1998**, *37* 1945–1948; c) T. M. Krygowski, M. K. Cyrañski, *Tetrahedron* **1999**, *55*, 11143–11148.

Received: November 13, 2006
Published online: January 31, 2007

